J Mater Sci (2011) 46:6835–6840
DOI 10.1007/s10853-011-5643-0

A simple synthesis of long nanostructured arrays of crystalline strontium titanates at low-temperatures

Liang Yin · Yunki Gwak · Choongho Yu

Received: 7 March 2011 / Accepted: 16 May 2011 / Published online: 1 June 2011

Abstract Long aligned arrays of crystalline strontium titanate ($SrTiO_3$) nanostructures were synthesized by using simple low-temperature processes that incorporate strontium into titanium oxides. Tubular nanostructures are often confine energy carriers that result in extraordinary transport behaviors in various semiconductors including strontium titanates, which are promising for developing efficient thermoelectric energy conversion materials. However, synthesizing a micron-to-milimeter scale array of one-dimensional ternary nanostructures has been difficult. Moreover, ternary compounds are often obtained as disordered cubic-shape particles at the end of complicated and/or long reactions. In this study, a two-step process—anodization for preparing amorphous titanium oxides and a subsequent thermal annealing process in a mixture of strontium hydroxide, ammonia, and water—was employed. Typical diameter and length of the tubes are $\sim$150 nm and $\sim$160 μm, respectively. It has been found that the amorphous structure of titanium oxides plays an important role in obtaining high-purity long strontium titanate nanotubes at low temperatures (90 and 180 °C) with short reaction times. Comparative and systematic studies with different sample pre-treatments, etching times, temperatures, reaction times, and strontium concentrations revealed reaction mechanisms and key synthesis parameters, which may be utilized to obtain other ternary or quaternary nanostructured compounds such as barium or lead titanates.

L. Yin · Y. Gwak · C. Yu (✉)
Mechanical Engineering Department, Texas A&M University, College Station, TX 77843, USA
e-mail: chyu@tamu.edu

C. Yu
Materials Science Engineering Program, Texas A&M University, College Station, TX 77843, USA

Introduction

Recent reports regarding extraordinary electrical and thermal transport properties of strontium titanates have attracted significant subsequent research efforts and debates related to the origin of such extraordinary behaviors [1–11]. For instance, the Seebeck coefficient could be increased without considerably sacrificing electrical conductivity by confining electron transport within nanoscale layers [4]. High electron mobility was observed from confined interfaces [5], and thermal conductivity was suppressed by introducing nanostructured oxygen vacancy clusters [2, 12]. These findings, in addition to the wide tunability in electrical and thermal transport properties of strontium titanates, have stimulated various transport related research including thermoelectricity [1–3]. These transport properties determine thermoelectric energy conversion efficiency, called as the thermoelectric figure of merit, $Z = S^2\sigma/k$, where S, σ, and k indicate the Seebeck coefficient (or thermopower), electrical conductivity, and thermal conductivity, respectively [13]. These properties are often strongly correlated, making Z enhancement extremely difficult. For example, in bulk materials, an increase of electrical conductivity often decreases the Seebeck coefficient and increases thermal conductivity. Such typical transport behaviors, however, could be altered when energy carriers are confined in low-dimensional nanostructures such as nanotubes and nanowires [14, 15].

Recently, ternary compound nanostructures have been synthesized by using various methods [16] including a molten-salt or sol–gel method for nanoparticles [17, 18], sol–gel methods for nanorods [19–21], a template method for nanotubes [22], and hydrothermal reactions for several days at relatively high temperatures to obtain nanowires/tubes [16, 23]. These nanostructures may not be suitable

for thermoelectric applications due to the inappropriate morphology such as cubic-shapes, short wires/tubes (a few hundreds of nanometer long), or/and other byproducts that are difficult to remove from strontium titanates. They are often clumped and dispersed in an arbitrary fashion, which requires a non-trivial assembly process to build practical materials. This article does not only present simple low-temperature synthesis methods to obtain arrays of strontium titanate nanostructures, but also provide a series of experimental studies for revealing reaction mechanisms. Comparative studies with different conditions elucidate key reactions to obtain pristine strontium titanates. The synthesis reaction involves a two-step process. First, tube arrays made of amorphous titanium oxides were synthesized by anodizing a titanium foil. Then, the amorphous tubes were converted into crystalline strontium titanates at either 90 °C or 180 °C with a beaker or pressure vessel in ambient air environment. This study may also provide useful information to synthesize other various ternary or/and quaternary titanates such as barium or lead titanates. The following describes experimental details of the synthesis method, key reaction mechanisms, and morphology/structure characterization.

Experimental details

Strontium titanate tube arrays were synthesized by incorporating strontium into tubular shape amorphous titanium oxides obtained by anodizing titanium foils. Before the anodization, titanium foils (purity 99.5%, ~250-μm thick) were ultrasonically cleaned in ethanol and de-ionized water. Then, the foil was immersed in a solution that contains 1.8 wt% de-ionized water, 0.3 wt% NH_4F, and 97.9 wt% ethylene glycol for anodization. When DC 60 V was applied between a titanium foil (anode) and a stainless steel foil (cathode), an array of nanotubes was formed from the outer surface to the center along the foil thickness direction. Typical size of the titanium foil was 20×5 mm^2 and the distance between the two foils was ~2 cm. The foils were typically anodized for 24 h in 100 mL solution, yielding tube arrays with a tube length of 100 μm or longer.

The tube array was further processed with various conditions to study reactions between strontium and titanium oxide tubes. The key reaction parameters including etching time, pre-treatment of the tubes, reaction temperature, reaction time, and strontium hydroxide ($Sr(OH)_2$) concentration were varied. In typical synthesis, the barrier layer of as-synthesized titanium oxide nanotubes were etched in a mixture of 0.1 M NH_4F and 0.1 M H_2SO_4 in water. Then, the samples were immersed in an ammonia solution (1 M in water) at 90 °C for 1 h. This process is necessary to remove fluorine adsorbed on the surface of the titanium oxide during the anodization and etching process. The nanotubes were then reacted in a mixture of 14 mL $Sr(OH)_2$ solution (0.1 M or 0.2 M in water) and 1 mL liquid ammonia (14.8 M in water) at either 90 °C in a beaker or 180 °C in a pressure vessel for 4 h or 12 h. The pH of the mixture was above 13. It is noted that the tube arrays were inserted in a separate bottle in the beaker or pressure vessel so as to avoid direct contact between the array and undissolved $Sr(OH)_2$.

Result and discussion

Figure 1 shows scanning electron micrographs (SEMs) and transmission electron micrographs (TEMs) of as-synthesized titanium oxide nanotubes. They are well aligned and vertically grown from the foil surface with diameters and length of ~150 nm and ~160 μm, respectively (Fig. 1a, b). A 0.25-mm thick Ti foil was completely anodized from both surfaces, creating two 160-μm-long nanotube layers separated by two thin barrier layers at the center. The volume expansion is due to the introduction of oxygen to titanium, forming amorphous titanium oxides. The diameter and length of the nanotubes can be altered by using different anodization voltage and anodization time [24, 25]. Gentle sonication of samples in an ultrasonic bath separated them into bundles and/or individual tubes for TEM analysis (Fig. 1c, d). The inset of Fig. 1d indicates the tube has an amorphous structure.

The amorphous titanium oxides underwent the fluorine desorption and subsequent strontium incorporation processes. Without the fluorine desorbing procedure, water insoluble SrF_2 (solubility: 0.0117 g per 100 mL water at 18 °C [15]) was crystallized, as indicated by X-ray diffraction (XRD) in Fig. 2a and b from nanotube samples reacted with 0.1 M $Sr(OH)_2$ at 90 °C or 180 °C for 2 h. Conversely, after the fluorine desorbing process, XRD peaks from SrF_2 disappeared, showing only crystalline $SrTiO_3$ from both 90 °C (Fig. 3a) and 180 °C (Fig. 3b) reactions. A typical SEM shown in Fig. 4a indicates tube shapes are well maintained after a strontium incorporation process with 0.1 M $Sr(OH)_2$ at 180 °C for 12 h. It was observed that some portions of the outer surface were covered with a layer of strontium titanates. In order to perform TEM analysis to identify the structure after reactions, the sample was sonicated in ethanol for a few seconds so as to break it into tiny pieces. It was impossible to inspect as-synthesized samples without sonication since the thickness of TEM samples should be ~100 nm or less. The ultrasonic power broke the brittle samples into small pieces as shown in Fig. 4b. The strontium incorporation increases the density and molar volume of the sample from

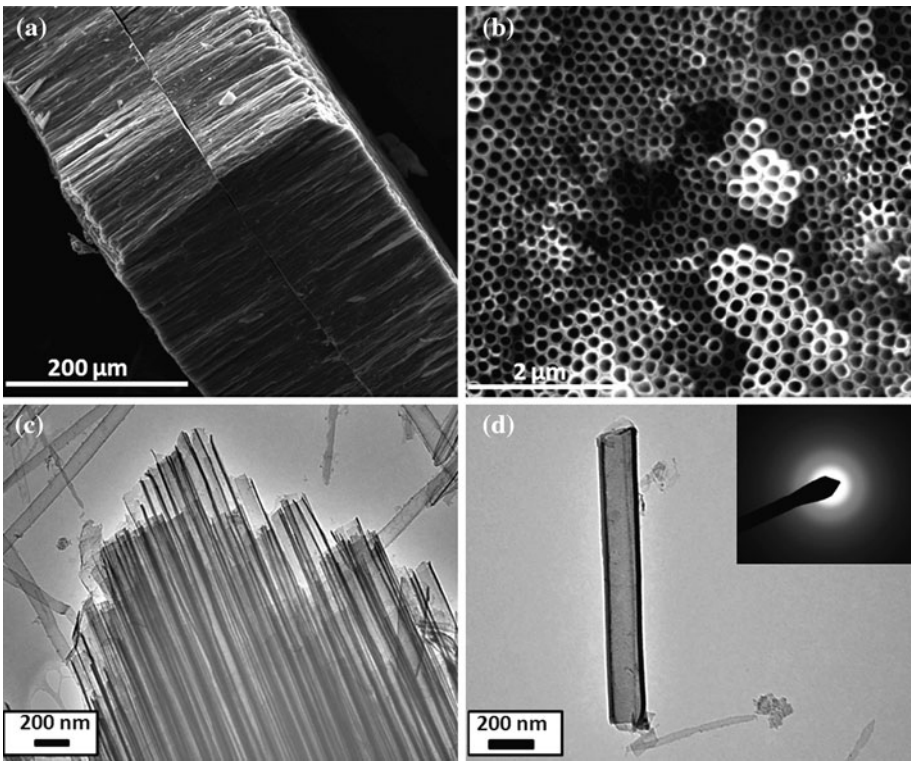

Fig. 1 **a** A cross section of a typical titanium oxide nanotube array by anodizing a titanium foil. Titanium oxide tubes were made from the outer surface to the center, creating a barrier layer that makes one of the tube ends closed. **b** An outer surface of the anodized foil shows circular pores from the tube array. Gentle sonication separated the array into **c** a bundle and **d** an individual titanium oxide nanotube. The electron diffraction in the *inset* of "**d**" indicates an amorphous structure

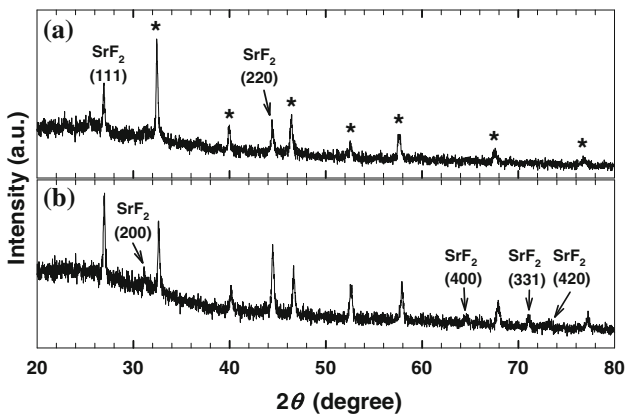

Fig. 2 Typical XRD scans of nanotube arrays after a strontium incorporation process with 0.1 M $Sr(OH)_2$ at (*a*) 90 °C and (*b*) 180 °C for 2 h without a fluorine desorbing process. Fluorine residues on the surface of titanium oxides from the anodization and etching processes are easily crystallized into SrF_2. Peaks indicated by "*" are from $SrTiO_3$

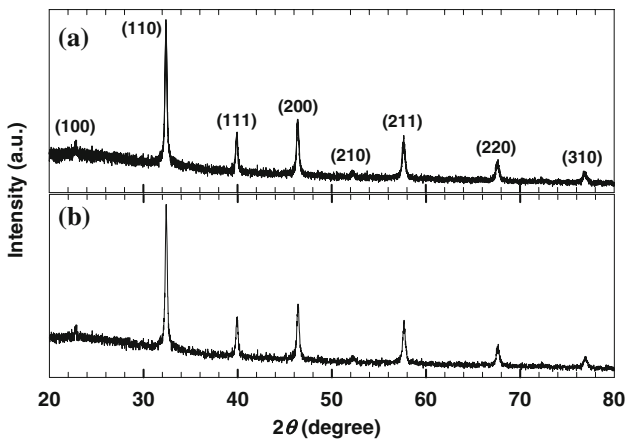

Fig. 3 Typical XRD scans of the tube array after a strontium incorporation process with 0.2 M $Sr(OH)_2$ at (*a*) 90 °C and (*b*) 180 °C for 4 h. Crystallographic planes indicate crystalline $SrTiO_3$

2.98 g/cm^3 and 26.80 cm^3/mol (amorphous titanium oxide) [26] to 5.13 g/cm^3 and 35.77 cm^3/mol (crystalline strontium titanate) [27], respectively. These differences between titanium oxides and strontium titanates may have made the wall thickness of the tubes non-uniform after strontium incorporation. The high resolution TEM image (Fig. 4c) and the selected area electron diffraction pattern (Fig. 4d) indicate a conversion from amorphous titanium oxides to crystalline strontium titanates with the axis in [100] direction. The spots other than the cubic structure in the SAED may be from the tiny spherical nanoparticles attached to the tube in Fig. 4b (e.g., the back side that is not shown in TEM). The nanoparticles are likely to come from broken pieces after a sonication process.

The relatively simple crystallization of ternary compounds is believed to be due to the amorphous structure of titanium oxides, allowing low reaction temperatures and short reaction time, as compared with other synthesis methods employing crystalline materials. In general,

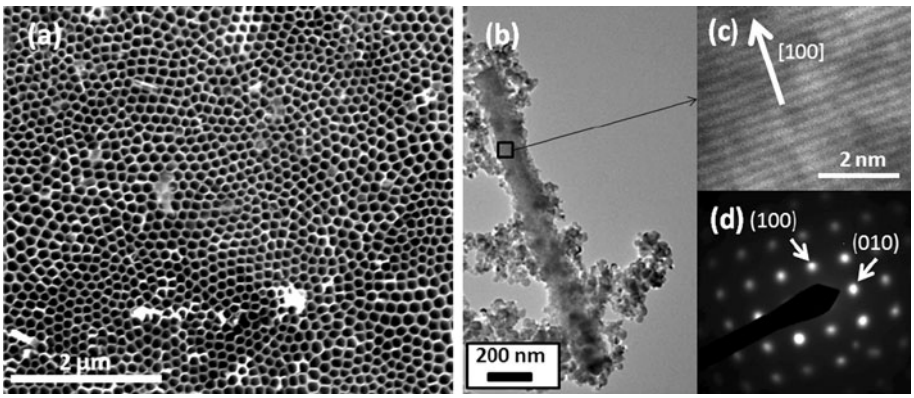

Fig. 4 **a** A strontium titanate tube array synthesized with 0.1 M $Sr(OH)_2$ at 180 °C for 12 h. **b** An individual strontium titanate nanostructure synthesized with 0.1 M $Sr(OH)_2$ at 90 °C for 4 h. **c** A high resolution image of a portion (marked with a *square* in "**b**") indicates crystalline strontium titanates with the axis in [100] direction. **d** An electron diffraction image corresponds to the image in "**c**"

low-temperature reactions often require a very long synthesis process or catalysts to overcome a reaction barrier. For example, a hydrothermal reaction with TiO_2 particles at 170 °C for 3 days produced approximately a few micron long clumped wires [23]. Byproducts are often inevitable despite a long time (20–60 h) reflux process with $SrCl_2$ and anatase TiO_2 [28]. In order to find the correlation between the crystallinity of titanium oxides and the reactivity of strontium with titanium oxides, the amorphous tubes were annealed before the strontium reaction at 450 °C for 2 h with ~20 sccm flow of oxygen in a 22-mm-diameter tube furnace. This annealing process converted amorphous structure (Fig. 5a, before annealing) into anatase TiO_2 (Fig. 5b), which is a well-known transformation upon annealing at elevated temperatures [29–32]. The annealed samples were reacted with a mixture of 14 mL $Sr(OH)_2$ (0.1 M in water) and 1 mL ammonia (14.8 M in water) for 4 h at 90 °C or 180 °C. XRD results (Fig. 5c, d) did not show prominent peaks comparable to those in Fig. 3 (crystalline strontium titanates). Furthermore, strontium was not identified from the tube array by using energy dispersive spectroscopy (EDS). In contrast, when the amorphous titanium oxide was reacted with strontium, the atomic ratio of Sr to Ti was approximately 1 to 1. This result suggests that the amorphous titanium oxide facilitates crystallization of ternary strontium titanates without requiring high temperatures and long reaction times. It is found that ammonia plays a role in retarding the crystallization of titanium oxides during the strontium incorporation process. When the amorphous titanium oxide is immersed in only water at either 90 °C or 180 °C for 2 h, it is possible to change the amorphous structure into anatase TiO_2, as indicated by XRD peaks in Fig. 6a and b. On the other hand, 1 M ammonia in water instead of only DI water kept the amorphous structure during both 2-h 90 °C and 180 °C reactions, as shown in Fig. 6c and d.

Finally, in order to confirm the conversion into strontium titanates from amorphous titanium oxides, samples were annealed after a strontium incorporation process in an oxygen flow (~20 sccm) at 450 °C for 2 h. Any remaining amorphous oxides will then crystallize. This would be due to the barrier layer or/and the deposition of crystallized strontium titanates on the sample surface, which may hinder strontium from being smeared into the pores. For this study, amorphous titanium oxides were etched in a mixture of 0.1 M NH_4F and 0.1 M H_2SO_4 for 0, 1.5, or 3.5 h so as to remove the barrier layer before a strontium

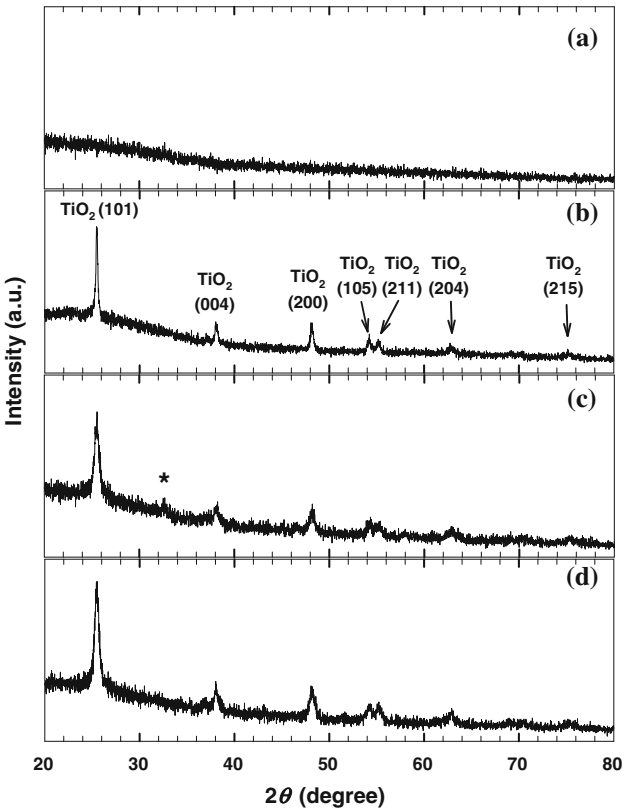

Fig. 5 Typical XRD scans of (*a*) amorphous titanium oxide nanotubes, (*b*) annealed titanium oxide nanotubes in a furnace with an oxygen flow at 450 °C for 2 h, and the nanotubes after strontium incorporation processes with 0.2 M $Sr(OH)_2$ (*c*) at 90 °C and (*d*) 180 °C for 4 h. The tiny peak near $2\theta = 32.4°$ (indicated by "*") would be from $SrTiO_3$

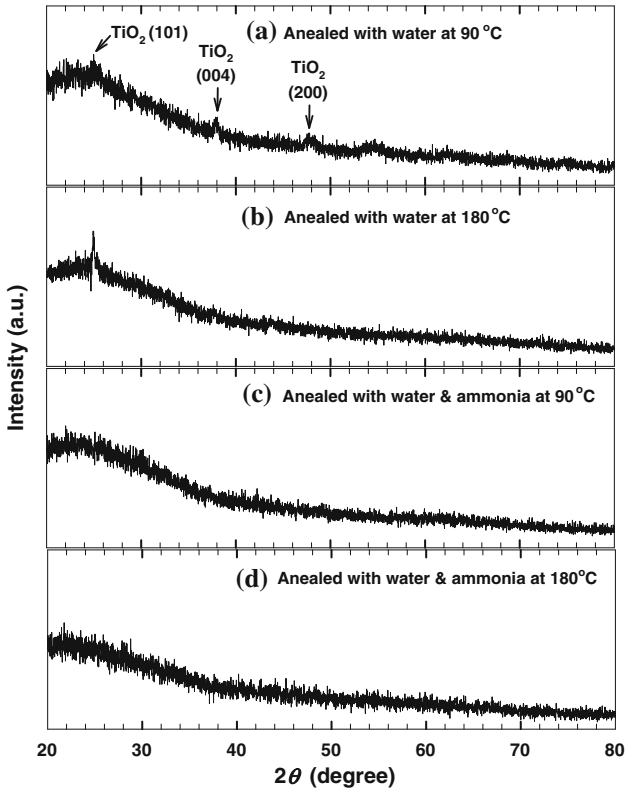

Fig. 6 Typical XRD scans of the amorphous titanium oxide nanotubes annealed in water at (*a*) 90 °C and (*b*) 180 °C for 2 h and ammonia (1 M in water) at (*c*) 90 °C or (*d*) 180 °C for 2 h

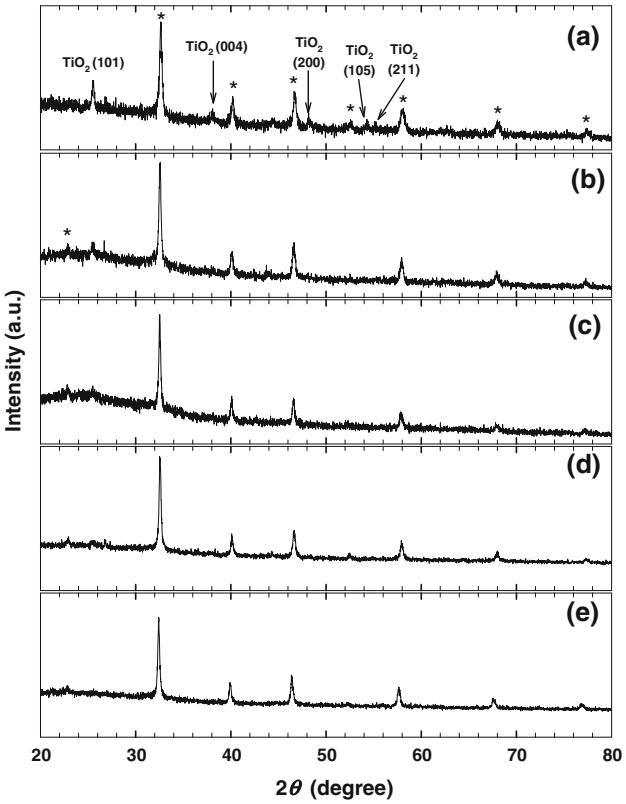

Fig. 7 Typical XRD scans of Samples 1–5 in Table 1 (corresponding scans are (*a*)–(*e*) in alphabetical order) after annealing in an oxygen flow (~20 sccm) at 450 °C for 2 h. Peaks indicated by "*" are from $SrTiO_3$

Table 1 Five different $SrTiO_3$ synthesis conditions to verify strontium incorporation into titanium oxides

Sample no.	Etching time (h)[a]	Reaction temp. (°C)	Reaction time for Sr incorporation (h)	$Sr(OH)_2$ concentration (M)
1	–	90	4	0.1
2	1.5	90	4	0.1
3	1.5	90	4	0.2
4	1.5	180	12	0.2
5	3.5	180	12	0.2

[a] After the etching process, fluorine was desorbed from the sample in 1 M ammonia solution at 90 °C before the strontium reaction

incorporation process, as listed in Table 1. The etch rate of the sample is estimated to be ~12.5 μm/h. It is noted that the pore side was etched much faster than the barrier side. Typical barrier layer thickness is several microns, and the total thickness of the sample is ~160 μm. When the titanium oxide tubes were reacted with 0.1 M $Sr(OH)_2$ at 90 °C for 4 h without etching the barrier layer, the titanium oxide was not fully converted into strontium titanates (Sample 1 in Table 1). After the oxygen annealing, anatase TiO_2 peaks appeared as shown in Fig. 7a. With an etching process for 1.5 h (Sample 2 in Table 1), XRD peaks corresponding to anatase TiO_2 were suppressed (Fig. 7b). On the other hand, an increase of strontium concentration (0.2 M $Sr(OH)_2$) (Sample 3 in Table 1) or a longer reaction (12 h) with a higher temperature (180 °C) (Sample 4 in Table 1) did not make significant changes in XRD, leaving tiny anatase TiO_2 peaks (Fig. 7c, d). After 3.5 h etching (Sample 5 in Table 1), anatase peaks were not identified anymore (Fig. 7e). This result suggests that amorphous titanium oxides have fully converted into strontium titanates. It is noted that all samples were crushed into a powder and dispersed on a glass substrate because x-ray scan depths are much shorter than the thickness of the samples.

Conclusion

Long aligned arrays of crystalline strontium-titanate nanostructures were successfully synthesized from amorphous titanium oxides with a simple reaction in a mixture of strontium hydroxide, ammonia, and water at 90 and 180 °C. Typical diameter and length of the tubes are ~150 nm and ~160 μm, respectively. It has been found

that the amorphous structure of the titanium oxides facilitates the strontium incorporation process even at low temperatures, producing high purity and long nanotubes with short reaction time. The low reaction temperatures and ammonia are believed to hinder crystallization of amorphous titanium oxides into anatase TiO_2, allowing low-temperature synthesis of strontium titanates. Comparative studies with different etching times, reaction temperatures and times, and $Sr(OH)_2$ concentration revealed that the reaction between the strontium and titanium oxides can be deterred by the barrier layers.

Acknowledgements This study was supported by the Thermal Transport Processes and the Solid State and Materials Chemistry Programs in the US National Science Foundation (Award No. 0854467), and the Pioneer Research Center Program through the National Research Foundation of Korea (Grant No. 2010-0002231) funded by the Ministry of Education, Science and Technology (MEST). The authors thank Yang for his assistance in acquiring XRD data.

References

1. Yu C, Scullin ML, Huijben M, Ramesh R, Majumdar A (2008) Appl Phys Lett 92:092118
2. Yu C, Scullin ML, Huijben M, Ramesh R, Majumdar A (2008) Appl Phys Lett 92:191911
3. Scullin ML, Yu C, Huijben M, Mukerjee S, Seidel J, Zhan Q, Moore J, Majumdar A, Ramesh R (2008) Appl Phys Lett 92:202113
4. Ohta H, Kim S, Mune Y, Mizoguchi T, Nomura K, Ohta S, Nomura T, Nakanishi Y, Ikuhara Y, Hirano M, Hosono H, Koumoto K (2007) Nat Mater 6:129
5. Ohtomo A, Muller DA, Grazul JL, Hwang HY (2002) Nature 419:378
6. Huijben M, Rijnders G, Blank DHA, Bals S, Van Aert S, Verbeeck J, Van Tendeloo G, Brinkman A, Hilgenkamp H (2006) Nat Mater 5:556
7. Thiel S, Hammerl G, Schmehl A, Schneider CW, Mannhart J (2006) Science 313:1942
8. Siemons W, Koster G, Yamamoto H, Harrison WA, Lucovsky G, Geballe TH, Blank DHA, Beasley MR (2007) Phys Rev Lett 98:196802
9. Brinkman A, Huijben M, Zalk MV, Huijben J, Zeitler U, Maan JC, Wiel WGVD, Rijnders G, Blank DHA, Hilgenkamp H (2007) Nat Mater 6:493
10. Kalabukhov A, Gunnarsson R, Borjesson J, Olsson E, Claeson T, Winkler D (2007) Phys Rev B 75:121404
11. Herranz G, Basletic M, Bibes M, Carretero C, Tafra E, Jacquet E, Bouzehouane K, Deranlot C, Hamzic A, Broto JM, Barthelemy A, Fert A (2007) Phys Rev Lett 98:216803
12. Muller DA, Nakagawa N, Ohtomo A, Grazul JL, Hwang HY (2004) Nature 430:657
13. Rowe DM (1995) CRC handbook of thermoelectrics. CRC Press, Boca Raton
14. Hochbaum AI, Chen R, Delgado RD, Liang W, Garnett EC, Najarian M, Majumdar A, Yang P (2008) Nature 451:163
15. Boukai AI, Bunimovich Y, Tahir-Kheli J, Yu JK, Goddard WA, Heath JR (2008) Nature 451:168
16. Mao Y, Park TJ, Zhang F, Zhou H, Wong SS (2007) Small 3:1122
17. Mao YB, Banerjee S, Wong SS (2003) J Am Chem Soc 125:15718
18. O'Brien S, Brus L, Murray CB (2001) J Am Chem Soc 123:12085
19. Urban JJ, Yun WS, Gu Q, Park H (2002) J Am Chem Soc 124:1186
20. Yang WD (1999) J Electron Mater 28:986
21. Jiang W, Gong X, Chen Z, Hu Y, Zhang X, Gong X (2007) Ultrason Sonochem 14:208
22. Luo Y, Szafraniak I, Nagarajan V, Wehrspohn RB, Steinhart M, Wendorff JH, Zakharov ND, Ramesh R, Alexe M (2003) Integr Ferroelectr 59:1513
23. Joshi UA, Lee JS (2005) Small 1:1172
24. Paulose M, Prakasam HE, Varghese OK, Peng L, Popat KC, Mor GK, Desai TA, Grimes CA (2007) J Phys Chem C 111:14992
25. Prakasam HE, Shankar K, Paulose M, Varghese OK, Grimes CA (2007) J Phys Chem C 111:7235
26. Gavrilov VY, Zenkovets GA, Kryukova GN (1998) In: Delmon B, Jacobs PA, Maggi R, Martens JA, Grange P, Poncelet G (eds) Preparation of catalysts VII, Elsevier, Amsterdam, p 609
27. Hellwege KH, Hellwege AM (1981) Landolt-Bornstein new series: group III, vol 16, Oxides. Springer-Verlag, New York, p 64
28. Mao YB, Banerjee S, Wong SS (2003) Chem Commun 408
29. Martin N, Rousselot C, Rondot D, Palmino F, Mercier R (1997) Thin Solid Films 300:113
30. Ouyang M, Bai R, Yang L, Chen Q, Han Y, Wang M, Yang Y, Chen H (2008) J Phys Chem C 112:2343
31. Dachille F, Simons PY, Roy R (1968) Am Miner 53:1929
32. Ovenstone J, Yanagisawa K (1999) Chem Mater 11:2770